Photovoltaic converters resistive parameters effect on its IV-curves and electroluminescence maps

© A.D. Malevskaya, M.A. Mintairov, V.V. Evstropov, D.A. Malevsky, R.A. Saliy, N.A. Kalyuzhny

loffe Institute,

194021 St. Petersburg, Russia E-mail: anmalevskaya@mail.ioffe.ru

Received May 5, 2025 Revised July 10, 2025 Accepted July 27, 2025

The IV-curves and electroluminescence (EL) maps of four AlGaAs/GaAs photovoltaic converters (PVCs) differing in the design of contact grids have been investigated. It is shown that EL map form comparative analysis allows to determine how the current flow process changes both inside the semiconductor layers (between the contact strips) and inside the metal contacts. The characteristics of all samples have been analyzed by a previously developed method with using the tube model of current flow. For all PVCs, saturation currents, sheet resistance, and resistance of metal contacts have been determined. The obtained values agreed with the differences incorporated in the design of PVC contact grids.

Keywords: photovoltaic converters, solar cells, spread resistance, contact resistance.

DOI: 10.61011/SC.2025.05.61991.8072

The development of photovoltaic converters (PVCs) of laser radiation for energy transmission systems is presently becoming a crucial task. To achieve high efficiency of such PVCs designed to convert high-power radiation [1–4], one needs to find a compromise between the magnitude of resistive losses and shading of the photoreceiving surface by the front contact grid. The design of front contacts of PVCs may be optimized by modeling the current spreading Various approaches to such modeling are known [5–8]. These include the tube model [8] used here, which is based on the concept of current tubes with their trajectory characterized by right-angle kinks. The advantage of this model is its physical simplicity and the possibility of experimental determination of its main parameters. The problem with application of current spreading models to experimental current-voltage curves (I-V curves) is that, as was demonstrated in [8], the parameters of resistance of the metal contact and the spreading layer have an equivalent effect on the I-V curve of a PVC. Therefore, the analysis of I-V curves only does not allow one to determine unambiguously the values of the spreading layer resistance and the metal contact resistance. In the tube model, these quantities are characterized by parameter R_{sheet} (spreading sheet resistance) or parameter R_L (characterizing the total lateral resistance of the structure), which depends on it, and parameter R_M (resistance of a metal strip). One solution to the mentioned problem is to perform an additional analysis of the electroluminescence (EL) map of the PVC surface [8,9]. EL map analysis is a well-known approach that allows one to judge the quality of PVC contacts (specifically, estimate resistive losses [10]). However, the influence of spreading sheet resistance and contact resistance on EL maps has not been studied in detail yet. In the present study, we examine thoroughly how the EL map of a PVC

changes depending on parameters R_M and R_L . The accuracy of determination of R_M and R_{sheet} by the methods developed earlier was also assessed.

EL maps and I–V curves were analyzed in accordance with the three-parameter tube model [8,9]. Let us give a brief general description of the approach to calculating the I–V curves and the EL map. In the model, the PVC surface enclosed between each pair of PVC contacts is divided into M parts. Each part is connected to the adjacent one by contact resistance R_M/M . Next, just as in [6], each part is divided further into N current tubes, each of them featuring a p-n junction and two resistances: vertical R_V and lateral. The lateral resistance depends on constant parameter R_L , which is specified by distance W between the contact strips and sheet resistance $R_{\rm sheet}$. The I–V curve of each PVC part is calculated using the formula

$$J = J_g - \Sigma \left(J_{0,tr,j} \exp \left(\frac{q[V - J \cdot R]}{A_j k_{\rm B} T} \right) \right), \tag{1}$$

where J is the current density, J_g is the photogenerated current, V is the applied voltage, $k_{\rm B}$ is the Boltzmann constant, T is the absolute temperature, q is the electron charge, $J_{0,tr,j} = \frac{J_{0,j}}{N \cdot M}$ are the saturation currents for current tubes, and A_j are the corresponding diode coefficients. According to the data from [9], resistance R is given by

$$R = R_V \cdot N \cdot M + R_L \cdot i \cdot M + \frac{1}{4} \cdot R_M \cdot k \cdot N \cdot S, \qquad (2)$$

where S is the sample area, i is the tube number, k is the contact part number, and R_M is calculated as

$$R_M = \frac{\rho_m}{W_m \cdot h_m} \cdot l_m, \tag{3}$$

where ρ_m is the resistivity of the contact metal and l_m , W_m , and h_m are the length, width, and height of a contact bus,

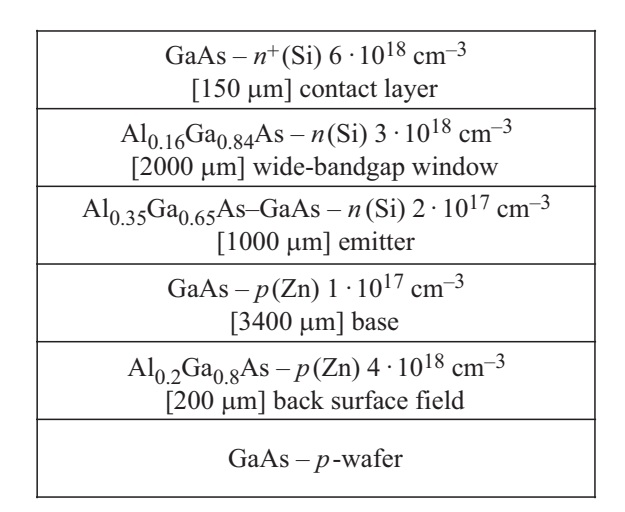


Figure 1. Diagram of the epitaxial PVC heterostructure.

respectively. Adding up the I-V curves for all parts of the photovoltaic converter determined using (1), one obtains the complete I-V curve of the PVC. Since the I-V curves are calculated separately for each part of the photovoltaic converter, one may find the voltages at the p-n junctions of all parts and, consequently, determine the distribution of EL intensity over the PVC surface. The EL intensity (L) of

each part is calculated by the formula

$$L = L_0 \exp\left(\frac{qV}{k_{\rm B}T}\right),\tag{4}$$

where L_0 is a pre-exponential factor.

The case considered in [8], where current is supplied to the edge of the PVC contact grid, is of interest in the study of the EL map. Analyzing the reduction in EL brightness with distance from the edge, one may then determine the characteristic quantities that affect the current spreading process. Precisely these characteristics and their variation with parameters R_L and R_M were investigated in the present study. For this purpose, we analyzed the I-V curves and EL maps of four AlGaAs/GaAs PVCs with parameters R_L and R_M varied by adjusting the distance between the PVC contacts (W = 100 and $140 \,\mu\text{m}$) and the geometry of contact strips $(W_m = 2 \mu m, h_m = 7 \mu m)$ and $W_m = 5 \,\mu\text{m}$, $h_m = 8 \,\mu\text{m}$), respectively. All four PVCs were made from a single structure grown by metalorganic vapor-phase epitaxy. The PVC structure is presented in Figure 1.

EL maps were studied within a wide range of currents passed through the PVC structure (from 0.1 to $20\,\mathrm{A/cm^2}$). Figure 2 presents the data obtained in measurements at 10 and $20\,\mathrm{A/cm^2}$). The recorded EL map changes were the most evident at these currents.

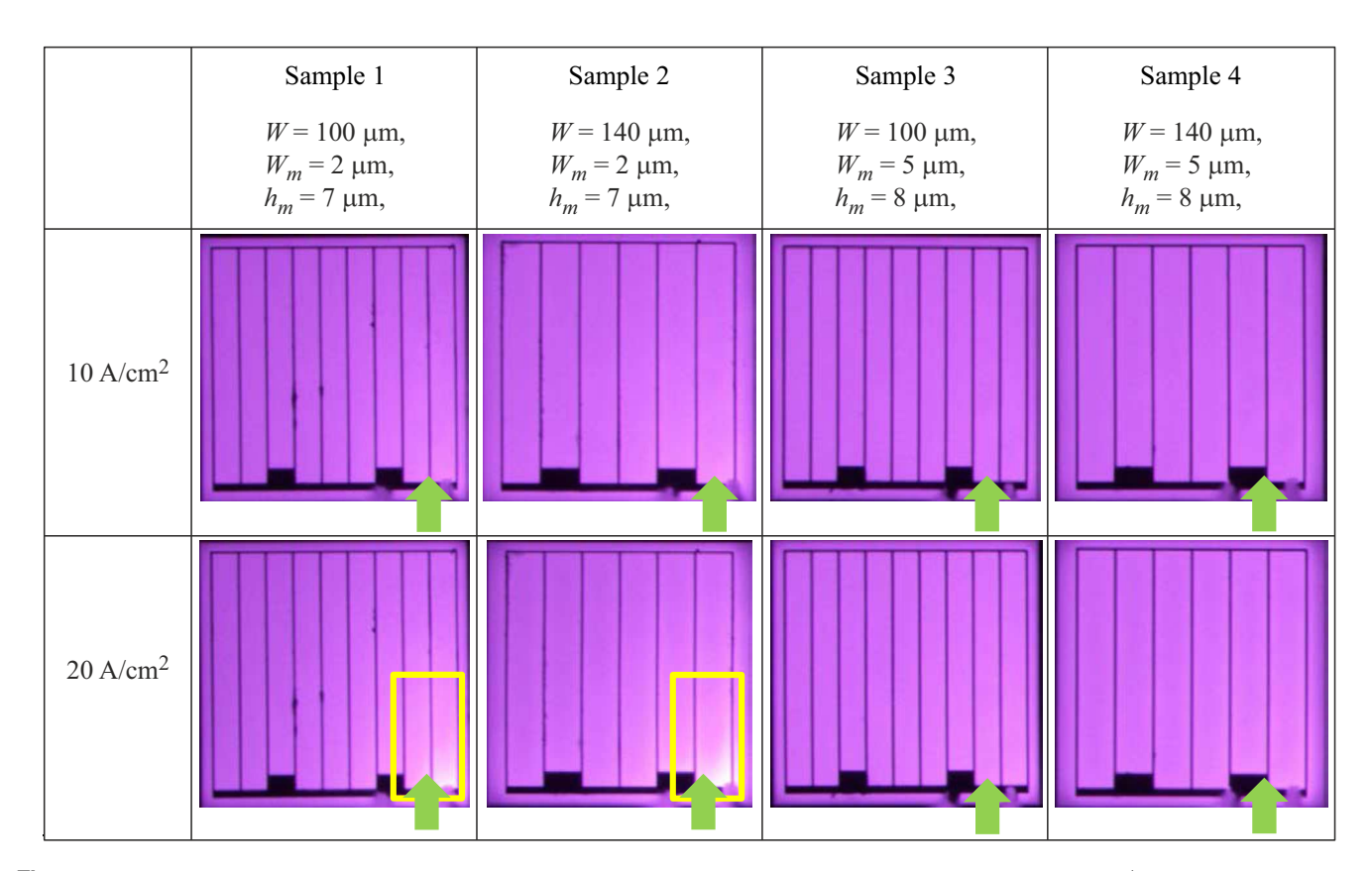


Figure 2. EL maps for PVC samples with a contact grid pitch of 100 and 140 μ m and two types of contact buses ($W_m = 2 \mu$ m, $h_m = 7 \mu$ m and $W_m = 5 \mu$ m, $h_m = 8 \mu$ m). The arrow denotes the contact connection site.

	Sample 1	Sample 2	Sample 3	Sample 4
	$W=100\mu\mathrm{m},$	$W=140\mu\mathrm{m},$	$W=100\mu\mathrm{m},$	$W=140\mu\mathrm{m},$
	$W_m = 7 \mu \mathrm{m},$	$W_m = 7 \mu \mathrm{m}$	$W_m = 8 \mu \mathrm{m},$	$W_m = 8 \mu\mathrm{m},$
	$h_m=2\mu\mathrm{m}$	$h_m=2\mu\mathrm{m}$	$h_m = 5 \mu\mathrm{m}$	$h_m = 5 \mu\mathrm{m}$
J_{01} , A/cm ²	$4.0 \cdot 10^{-7}$	$3.0 \cdot 10^{-7}$	$3.0 \cdot 10^{-7}$	$3.0 \cdot 10^{-7}$
$J_{01.5}$, A/cm ²	$1.4 \cdot 10^{-13}$	$1.0 \cdot 10^{-13}$	$1.05 \cdot 10^{-13}$	$1.0 \cdot 10^{-13}$
J_{02} , A/cm ²	$7.0 \cdot 10^{-11}$	$1.0 \cdot 10^{-10}$	$1.0 \cdot 10^{-10}$	$1.0 \cdot 10^{-10}$
$R_{\rm sheet}$, Ohm · cm ²	12.20	12.75	12.0	12.24
R_V , Ohm	0.0			
R_M , Ohm	1.20	0.99	0.35	0.40

Results of approximation of EL maps and I-V curves of the studied AlGaAs/GaAs PVC samples

Note. J_{01} , $J_{01.5}$, and J_{02} are the saturation currents with ideality factors A=1, 1.5, and 2; R_V is the vertical resistance of the structure; R_M is the contact bus resistance (the bus length is 0.1 cm); and R_{sheet} is the spreading sheet resistance that is calculated as $R_{\text{sheet}} = R_L h_s / (W/2)^2$ [6], where h_s is the thickness of the current spreading region (in the examined samples, $h_s = 3 \,\mu\text{m}$).

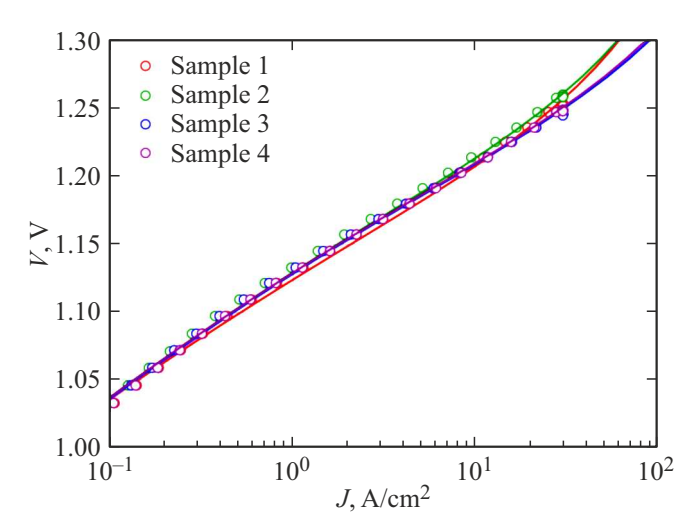


Figure 3. I–V curves of the studied AlGaAs/GaAs PVC samples. Symbols — experimental dark I–V curves; solid lines — results of approximation by the tube model.

A comparison of the EL maps of samples 1 and 2 at a current of $20 \, \text{A/cm}^2$ reveals the influence of parameter R_L . This is seen most clearly in the region highlighted by a yellow rectangle in Figure 1. Specifically, sample 1 (with a lower R_L due to a smaller distance between contacts W) has a more uniform distribution of the EL intensity within the strip closest to the PVC edge. In contrast, the current in sample 2 with a higher R_L flows predominantly along the rightmost contact strip, which is less pronounced in sample 1. Thus, the R_L reduction is manifested through a more uniform glow map between two contact strips.

A comparison of the EL maps of samples 1 and 2 with samples 3 and 4 reveals the influence of parameter R_M . At both currents, a more uniform distribution of EL intensity is observed in samples 3 and 4 that have a lower contact resistance R_M due to a larger cross section of contacts (their width and height were 5 and 8 μ m, respectively, while the corresponding values for samples 1 and 2 were 2 and 7 μ m).

Thus, the R_M reduction is manifested through an increase in uniformity of the EL intensity of the entire PVC surface.

The use of the tube model and the method from [7,8] for analysis of the EL maps (Figure 2) and the I–V curves (Figure 3) provided an opportunity to determine parameters R_L and R_M for the studied samples. The method is based on adjustment of model parameters via approximation of both the I–V curve and the attenuation of EL intensity of the strips near the contacts (Figure 4). Note that expression (2) is valid for the I–V curves obtained under such conditions that ensure a uniform flow of current to all contact strips. Since current in the presented experiment was supplied to the edge of the contact grid, the coefficient (1/4) found in expression (2) should change. Its value of 1/8 was determined empirically. The obtained model parameters are listed in the table.

The determined R_{sheet} parameters (spreading sheet resistance) vary only slightly between different AlGaAs/GaAs PVC samples. The theoretical estimate of the same parameter is similar: $R_{\text{sheet}} = 12 \Omega$. In contrast the obtained values of R_M deviate from the theoretical estimate, which was 1.41Ω for samples 1 and 2 and 0.49Ω for samples 3 and 4. The observed discrepancy may be attributed to differences between the actual and design contact sizes $(\sim 0.4 \,\mu\text{m} \text{ for samples 1 and 2; } \sim 1.0 \,\mu\text{m} \text{ for samples 3}$ and 4) or to an unaccounted resistance at the metalsemiconductor interface. Notably, the obtained data reveal that resistance R_M of samples 3 and 4 is, on average, 2.95 times lower than the resistance of samples 1 and 2. This value agrees closely with the theoretical estimate of 2.87. All calculations yielded a near-zero R_V value, indicating that its contribution to the total resistive losses is significantly smaller than the contribution of R_L and R_M . Note also that the resistance of metal contacts differs in pairs of samples 1–2 and 3–4, although the values of geometric parameters in these pairs are equal. This is likely attributable to the presence of a larger number of defects (in the form of dark spots on the EL maps near the contact buses) in samples 1 and 4 (Figure 2). This suggests that the method of examination of the I-V curves and EL maps with the use

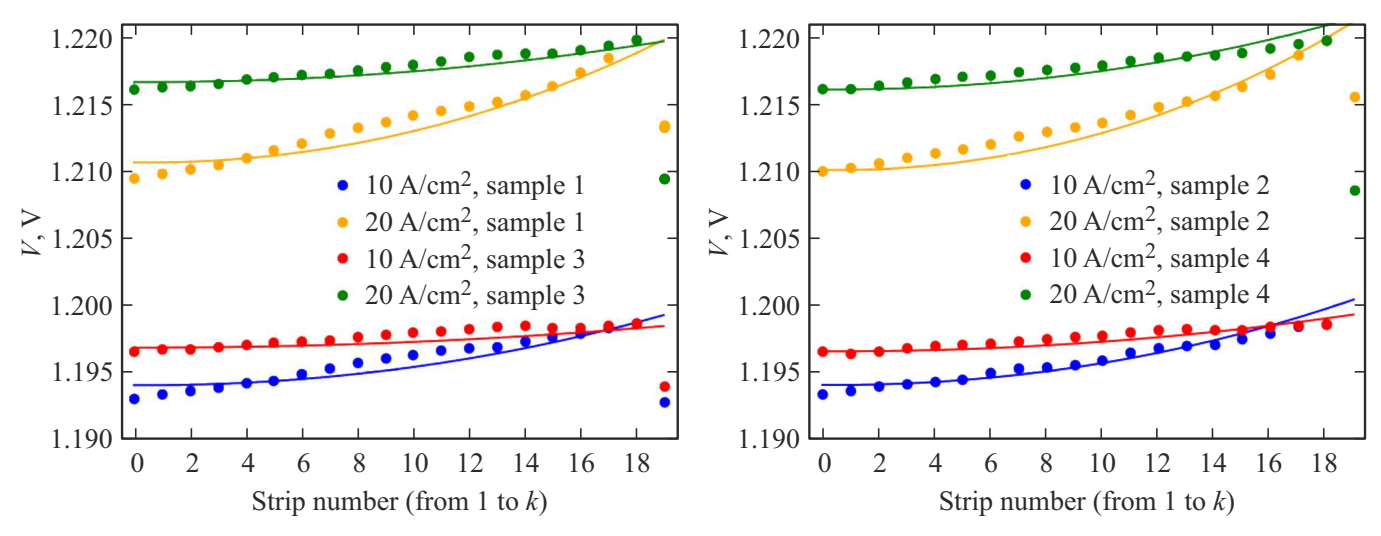


Figure 4. Attenuation of the EL intensity of strips. Dots and lines represent the experimental data and the results of approximation, respectively.

of the tube model allows one to determine sheet resistance $R_{\rm sheet}$ with high accuracy, perform a comparative analysis of several samples, and determine the magnitude of difference between their metal bus resistances. The proposed method ensures effective characterization of resistive losses and provides an opportunity to model the current distribution in PVCs.

- [9] T. Trupke, R.A. Bardos, M.C. Schubert, W. Warta. Appl. Phys. Lett., 89 (4), 44107 (2006).
- [10] T. Fuyuki, H. Kondo, T. Yamazaki, Y. Takahashi, Y. Uraoka. Appl. Phys. Lett., 86 (26), 262108 (2005).

Translated by D.Safin

Conflict of interest

The authors declare that they have no conflict of interest.

References

- Z.I. Alferov, V.M. Andreev, V.D. Rumyantsev. In: *High-Efficient Low-Cost Photovoltaics*, ed. by V. Petrova-Koch, R. Hezel, A. Goetzberger (Cham., Springer, 2020), Springer Ser. Opt. Sci., v. 140, p. 133.
- [2] M. Steiner, S.P. Philipps, M. Hermle, A.W. Bett, F. Dimroth. Progr. Photovolt.: Res. Appl., 19 (1), 73 (2011).
- [3] H. Helmers, Ed. Oliva, M. Schachtner, G. Mikolasch, L.A. Ruiz-Preciado, Al. Franke, J. Bartsch. Progr. Photovolt.: Res. Appl., 32 (9), 636 (2024).
- [4] C. Algora, I. García, M. Delgado, R. Peña, C. Vá zquez, M. Hinojosa, I. Rey-Stolle. Joule, 6 (2), 340 (2022).
- [5] B. Galiana, C. Algora, I. Rey-Stolle. Progr. Photovolt.: Res. Appl., 16, 331 (2008).
- [6] M.A. Mintairov, V.V. Evstropov, S.A. Mintairov, N.Kh. Timoshina, M.Z. Shvarts, N.A. Kalyuzhnyy. Semiconductors, 50 (7), 970 (2016).
- [7] A.D. Malevskaya, M.M. Mintairov, V.V. Evstropov, D.A. Malevskiy, A.V. Malevskaya, N.A. Kalyuznyy. St. Petersburg State Polytech. Univ. J. Phys. Math., 18 (1.1), 111 (2025).
- [8] A.D. Malevskaya, M.A. Mintairov, V.V. Evstropov, D.A. Malevskiy, N.A. Kalyuzhnyy. Semiconductors, 58 (10), 528 (2024).